Free Energy Calculations: An Efficient Adaptive Biasing Potential Method

Bradley M. Dickson,*,†,‡ Frédéric Legoll,§ Tony Lelièvre,† Gabriel Stoltz,† and Paul Fleurat-Lessard*,‡

Université Paris Est, CERMICS, Project MICMAC Ecole des Ponts ParisTech - INRIA, 6 & 8 Avenue Blaise Pascal, 77455 Marne-la-Vallée Cedex 2, France, Université de Lyon, Laboratoire de Chimie UMR 5182, École Normale Supérieure de Lyon, 46 allée d'Italie, 69364 Lyon Cedex 7, France, and Université Paris Est, Institut Navier, LAMI, Project MICMAC Ecole des Ponts ParisTech - INRIA, 6 & 8 Avenue Blaise Pascal, 77455 Marne-la-Vallée Cedex 2, France

Received: January 31, 2010; Revised Manuscript Received: March 13, 2010

We develop an efficient sampling and free energy calculation technique within the adaptive biasing potential (ABP) framework. By mollifying the density of states we obtain an approximate free energy and an adaptive bias potential that is computed directly from the population along the coordinates of the free energy. Because of the mollifier, the bias potential is "nonlocal", and its gradient admits a simple analytic expression. A single observation of the reaction coordinate can thus be used to update the approximate free energy at every point within a neighborhood of the observation. This greatly reduces the equilibration time of the adaptive bias potential. This approximation introduces two parameters: strength of mollification and the zero of energy of the bias potential. While we observe that the approximate free energy is a very good estimate of the actual free energy for a large range of mollification strength, we demonstrate that the errors associated with the mollification may be removed via deconvolution. The zero of energy of the bias potential, which is easy to choose, influences the speed of convergence but not the limiting accuracy. This method is simple to apply to free energy or mean force computation in multiple dimensions and does not involve second derivatives of the reaction coordinates, matrix manipulations nor on-the-fly adaptation of parameters. For the alanine dipeptide test case, the new method is found to gain as much as a factor of 10 in efficiency as compared to two basic implementations of the adaptive biasing force methods, and it is shown to be as efficient as well-tempered metadynamics with the postprocess deconvolution giving a clear advantage to the mollified density of states method.

1. Introduction

Many interesting physical systems can be categorized as rare-event systems. The uniting feature of these systems is that the dynamics involved require a time resolution much smaller than the time scale on which interesting events take place. Of central importance to the evolution of such systems is the free energy. Low lying regions of the free energy and the barriers separating these regions dictate the thermodynamics and, to some extent, the kinetics[1] of the system. Because free energy barriers are only rarely crossed, efficient exploration of the free energy landscape is practically impossible with straightforward integration of the equations of motion.

Recently, a number of approaches have used generalized ensemble simulations to accelerate exploration of the free energy landscape.[2−14] In these methods, information about the free energy is estimated during simulation, and that information is fed back to the dynamics as a statistical bias. While there are many variations on this idea, the common aim is to minimize the time spent sampling regions of the free energy that have been sampled in the past. These schemes may be classified into two categories: adaptive biasing force (ABF) methods,[7,15] which use an approximation of the mean force to bias the dynamics, and adaptive biasing potential (ABP) methods,[2,6,8,9,13,14] which use an approximation of the free energy as a bias potential.

The underlying idea for all adaptive methods is that it is computationally more efficient to sample the distribution associated with a flattened free energy than it is to sample the density associated with the actual, very rough free energy. In the spirit of the work of Berg et al.,[2] Wang and Landau,[5,6] Eisenmenger et al.,[4,16] and Procacci et al.,[9] we propose an ABP method that builds an approximate density of states (DOS) and uses that approximation to define a bias potential. However, in contrast to these approaches, we use a mollification of the underlying DOS to produce the desired approximation. This leads to a smooth, adaptive bias potential whose gradient admits a simple analytic expression and that can be computed without knowledge of the actual DOS. Because the actual and approximate free energies are related by a convolution, it is easy to recover the former from the latter via deconvolution. Our framework is not restricted to one-dimensional or orthogonal reaction coordinates. Moreover, it avoids second derivatives of the reaction coordinate.

This paper is organized as follows. We describe our ABP method in section 2 (see, in particular, eqs 9, 10, and 11), and comment on its convergence. We contrast this method to existing ones in section 3, and present some numerical validation on a benchmark system in section 4. Our conclusions are summarized in section 5.

* To whom correspondence should be addressed. E-mail: adynata@gmail.com, Paul.Fleurat-Lessard@ens-lyon.fr.
† Université Paris Est, CERMICS.
‡ Université de Lyon.
§ Université Paris Est, Institut Navier.

10.1021/jp100926h
Published on Web 04/09/2010

2. Description of the Method

2.1. Free Energy and Its Mollified Version. Consider a system whose configuration is described by a variable $x \in \mathcal{X}$, where $\mathcal{X}$ is the configuration space. We denote by V the potential energy function. Assume that we are given an N-dimensional reaction coordinate $\xi(x)$ with values in Ω, which characterizes some physical event. The DOS at a value ξ^* of the reaction coordinate is defined as

$$e^{-\beta A(\xi^*)} = Z^{-1} \int_{\mathcal{X}} \delta(\xi(x) - \xi^*) e^{-\beta V(x)} \, dx \qquad (1)$$

where $\beta = 1/k_B T$, and Z is a normalization constant, chosen such that

$$\int_{\Omega} e^{-\beta A(\xi)} \, d\xi = 1$$

Equation 1 defines the free energy $A(\xi^*)$. Recall that, in practice, the free energy needs only be known up to an additive constant since the important quantities to describe the relative likelihoods of physical states are free-energy differences.

In general, the free energy is unknown and has to be approximated. The method we propose in this work is based on the following limit:

$$e^{-\beta A(\xi^*)} = \lim_{\alpha \to 0} e^{-\beta A_\alpha(\xi^*)}$$

where

$$e^{-\beta A_\alpha(\xi^*)} = Z^{-1} \int_{\mathcal{X}} \delta_\alpha(\xi(x) - \xi^*) e^{-\beta V(x)} \, dx \qquad (2)$$

with, for instance, a Gaussian approximation of the Dirac delta function:

$$\delta_\alpha(\xi) = \left(\frac{1}{\alpha\sqrt{\pi}}\right)^N \exp\left(-\frac{|\xi|^2}{\alpha^2}\right)$$

Equation 2 defines an approximate free energy A_α, obtained by sampling the DOS at a finite α, i.e., by sampling a mollified DOS. Notice that the approximation resulting from finite α can in fact be rewritten as a convolution of the actual DOS $e^{-\beta A}$ with δ_α. Indeed,

$$\begin{aligned} e^{-\beta A_\alpha(\xi^*)} &= Z^{-1} \int_{\mathcal{X}} \delta_\alpha(\xi(x) - \xi^*) e^{-\beta V(x)} \, dx \\ &= Z^{-1} \int_{\Omega} \int_{\mathcal{X}} \delta_\alpha(\bar{\xi} - \xi^*) \delta(\xi(x) - \bar{\xi}) e^{-\beta V(x)} \, dx \, d\bar{\xi} \\ &= \int_{\Omega} \delta_\alpha(\bar{\xi} - \xi^*) e^{-\beta A(\bar{\xi})} \, d\bar{\xi} \end{aligned} \qquad (3)$$

This remark is the basis for an extraction of the actual free energy A from A_α through a deconvolution procedure (see section 4.1). While we make this presentation with a scalar α, this could easily be generalized to the case where α takes different values in different dimensions of the reaction coordinate.

Equation 3 is also helpful in assessing the errors introduced in simulations employing harmonic constraint potentials to compute the free energy. The corresponding error is analogous to the convolution errors discussed in this paper. Note that the parameter α can be converted to a force constant for a harmonic potential via $k = 2k_B T/\alpha^2$, where k is the force constant. Errors resulting from finite k can be identified as resulting from a convolution between the true DOS and a known Gaussian function. Typically, the harmonic constraints are tight enough for A_α to be a good approximation of A, but any persisting bias can, at least in principle, be removed by deconvolution as shown below.

2.2. Interest of the Mollified Free Energy. In this work, we use A_α to define an adaptive bias. The first interest of this approach is that the gradient of A_α is much easier to compute than the gradient of A. Indeed, the latter reads (see refs 17−19)

$$F_j(\xi^*) = \left\langle \sum_{i=1}^{N} \nabla V \cdot G_{ji}^{-1} \nabla \xi_i - \beta^{-1} \nabla \cdot (G_{ji}^{-1} \nabla \xi_i) \right\rangle_{\xi^*} \qquad (4)$$

where $\langle \cdot \rangle_{\xi^*}$ denotes a canonical average for a fixed value of the reaction coordinate, and G is the Gram matrix. The latter matrix is defined as $G = JJ^t$ with $J_{ij} = \partial \xi_i / \partial x_j$ (x_i are the Cartesian coordinates on which the reaction coordinates are defined). The computation of the free energy gradient therefore requires the computation of second derivatives of the reaction coordinate, which is cumbersome in many cases. The gradient of the mollified free energy has a much simpler expression:

$$\frac{\partial A_\alpha(\xi^*)}{\partial \xi_j^*} = -k_B T \frac{\int_{\mathcal{X}} \partial_{\xi_j^*} \delta_\alpha(\xi(x) - \xi^*) e^{-\beta V(x)} \, dx}{\int_{\mathcal{X}} \delta_\alpha(\xi(x) - \xi^*) e^{-\beta V(x)} \, dx} \qquad (5)$$

where j is a reaction coordinate index and

$$\partial_{\xi_j^*} \delta_\alpha(\xi_j(x) - \xi^*) = \frac{2}{\alpha^2} (\xi_j(x) - \xi_j^*) \delta_\alpha(\xi(x) - \xi^*)$$

In particular, no derivative of the reaction coordinates are required.

Another interest of the mollified free energy lies in the nonlocality of δ_α, which allows a single observation of ξ to contribute to A_α for a range of values ξ^*, leading to a faster convergence. The question is then whether there is a range of α for which (i) α is sufficiently large so that A_α could be estimated with fewer samples than what would be required to compute A and (ii) α is sufficiently small, so that A_α is close enough to A to efficiently bias the dynamics. We show in section 4.3 that a large range of α satisfies these two conditions on a paradigmatic test case.

2.3. A New ABP Method. ***2.3.1. Construction of the Method.*** To compute approximations of eqs 3 and 5 as time averages along a trajectory x_t driven by the potential function $V(x)$, we first assume that x_t is ergodic with respect to the canonical ensemble. We may take x_t as a solution to the Langevin equation driven by the potential V, for example. Using trajectory averages, eq 3 can be approximated by the following longtime limit:

$$e^{-\beta A_\alpha(\xi^*, t)} = Z_t^{-1} \left(1 + \int_0^t \delta_\alpha(\xi(x_s) - \xi^*) \, ds\right) \qquad (6)$$

where the normalization constant Z_t is

$$Z_t = \int_\Omega (1 + \int_0^t \delta_\alpha(\xi(x_s) - \xi^*)\, \mathrm{d}s)\, \mathrm{d}\xi^* = |\Omega| + t$$

The normalization constant ensures that

$$\int_\Omega \mathrm{e}^{-\beta A_\alpha(\xi,t)}\, \mathrm{d}\xi = 1 \tag{7}$$

at all times $t \geq 0$. Notice that we implicitely assumed that the reaction coordinate has values in a finite space Ω. This is indeed the case when angles are considered. For unbounded reaction coordinates, it is always possible to restrict the sampling to important values of $\xi(x)$. In practice, the range of the reaction coordinate needs to be truncated anyway.

From eq 6, we obtain

$$\frac{\partial A_\alpha(\xi^*, t)}{\partial \xi_j^*} = -k_\mathrm{B}T \frac{\int_0^t \partial_{\xi_j^*}\delta_\alpha(\xi(x_s) - \xi^*)\, \mathrm{d}s}{1 + \int_0^t \delta_\alpha(\xi(x_s) - \xi^*)\, \mathrm{d}s} \tag{8}$$

which, in the longtime limit converges to eq 5.

Now, a simple ergodic average such as eq 6 or eq 8 can of course not be used in practice since the dynamics at hand are usually metastable for complex systems, and the convergence of the time averages eq 6 and eq 8 is very slow. We therefore need to bias the dynamics in order to remove the metastability.

In what follows, we will consider a trajectory x_t obtained from the equations of motion with the biased potential $V + V_\mathrm{b}$. The idea behind adaptive method is to use the opposite of some current approximation of the free energy as a biasing potential, and to update the estimate as time goes on, in a way such that the bias eventually converges to the correct free energy. Here, we consider an ABP method, defined through the following update of the biasing potential V_b:

$$\mathrm{e}^{\beta V_\mathrm{b}(\xi,t)} = \mathrm{e}^{-\beta \Delta A_\alpha(\xi,t)} \mathrm{e}^{\beta c} \tag{9}$$

where the renormalized current approximation of the mollified free energy $\mathrm{e}^{-\beta \Delta A_\alpha(\xi,\, t)}$ is

$$\mathrm{e}^{-\beta \Delta A_\alpha(\xi,t)} = \frac{\mathrm{e}^{-\beta A_\alpha(\xi,t)}}{\max_{\xi^*}[\mathrm{e}^{-\beta A_\alpha(\xi^*,t)}]}$$

The parameter c in eq 9 is an important quantity in our method, which allows one to tune the convergence rate of the method. We discuss its choice in section 2.3.3. With these definitions, $V_\mathrm{b} = -A_\alpha$ up to an additive constant that is chosen such that $\max[V_\mathrm{b}] = c$. Similarly, $\Delta A_\alpha = A_\alpha$, again, up to an additive constant that is such that $\min\,[\Delta A_\alpha] = 0$.

Departing from standard ABP/ABF frameworks, we use ideas from importance sampling to write eqs 6 and 8 as time averages over biased trajectories

$$\mathrm{e}^{-\beta A_\alpha(\xi^*,t)} = Z_t^{-1}\Big(1 + \int_0^t \delta_\alpha(\xi(x_s) - \xi^*)\mathrm{e}^{\beta V_\mathrm{b}(\xi(x_s),s)}\, \mathrm{d}s\Big) \tag{10}$$

where Z_t is still a normalization constant ensuring eq 7, and

$$\frac{\partial A_\alpha(\xi^*, t)}{\partial \xi_j^*} = -k_\mathrm{B}T \frac{\int_0^t \partial_{\xi_j^*}\delta_\alpha(\xi(x_s) - \xi^*)\mathrm{e}^{\beta V_b(\xi(x_s),s)}\, \mathrm{d}s}{1 + \int_0^t \delta_\alpha(\xi(x_s) - \xi^*)\mathrm{e}^{\beta V_\mathrm{b}(\xi(x_s),s)}\, \mathrm{d}s} \tag{11}$$

The ABP method we discuss here is based on the biasing potential eq 9, updated with the current estimate of the free energy eq 10. New configurations are obtained by integrating in time the biased equations of motion using the simple estimate eq 11 for the biasing force. The convergence of this method is discussed in section 2.3.3.

In fact, eq 10 is a way to evaluate the convolution in eq 3 at each point ξ^* using a biased trajectory. This gives us a precise understanding of how using finite α introduces error in the estimate A_α and how to remove that error. This is a strength of our method. If we try to draw analogy with metadynamics, the framework of eq 10 would imply the continuous deposition of the Gaussians δ_α at each point $\xi(x_t)$ along the trajectory. Notice that, in this analogy, the Gaussians would be added to the DOS rather than to the bias potential, precluding us from going any further with the analogy.

2.3.2. Time Discretization. Let us briefly discuss the time discretization of the method based on eqs 9, 10, and 11. Assume that we have a suitable discretization where time is broken into parts of duration Δt so that $t = n\Delta t$ and $x_{i\Delta t}$ is written x_i. The biasing potential is now updated as

$$\mathrm{e}^{\beta V_\mathrm{b}(\xi,n)} = \mathrm{e}^{-\beta \Delta A_\alpha(\xi,n)} \mathrm{e}^{\beta c} \tag{12}$$

where $\mathrm{e}^{-\beta \Delta A_\alpha(\xi,\, n)} = \mathrm{e}^{-\beta A_\alpha(\xi,\, n)}/\max_{\xi^*}[\mathrm{e}^{-\beta A_\alpha(\xi^*,\, n)}]$, and eqs 10 and 11 are respectively replaced by

$$\mathrm{e}^{-\beta A_\alpha(\xi^*,n+1)} = Z_n^{-1}\left(1 + \sum_{i=0}^{n} \delta_\alpha(\xi(x_i) - \xi^*)\mathrm{e}^{\beta V_\mathrm{b}(\xi(x_i),i)}\right) \tag{13}$$

and

$$\frac{\partial A_\alpha(\xi^*, n+1)}{\partial \xi_j^*} = k_\mathrm{B}T \frac{\sum_{i=0}^{n} \partial_{\xi_j^*}\delta_\alpha(\xi(x_i) - \xi^*)\mathrm{e}^{\beta V_\mathrm{b}(\xi(x_i),i)}}{1 + \sum_{i=0}^{n} \delta_\alpha(\xi(x_i) - \xi^*)\mathrm{e}^{\beta V_\mathrm{b}(\xi(x_i),i)}} \tag{14}$$

At $t = 0$ we have $\exp[-\beta A_\alpha(\xi, 0)] = 1/Z_0$. Let us emphasize again that the trajectory x_i is generated from a biased equation of motion associated with the biased potential $V + V_\mathrm{b}$.

The implementation only requires storing the current value of the numerator and denominator of eq 14 at the points ξ^*. In particular, Z_n is never needed in practice (see Appendix A). The biasing force $-\nabla V_\mathrm{b}$, needed for instance to integrate the Langevin dynamics, is obtained through eq 14.

2.3.3. Convergence and Consistency. It can be checked that, if the biasing potential V_b converges in the long-time limit, then it converges to $-A_\alpha$ up to an additive constant. Indeed, denoting by $\bar{A}_\alpha(\xi) = \lim_{t\to+\infty} A_\alpha(\xi, t)$, the trajectory x_i is sampled according to the limiting canonical measure associated with the potential $V - \bar{A}_\alpha + C$ (where C is an unimportant constant), so that eq 10 leads to

$$e^{-\beta\bar{A}_\alpha(\xi^*)} = \lim_{t\to+\infty} \frac{1 + \int_0^t \delta_\alpha(\xi(x_s) - \xi^*)e^{\beta V_b(\xi(x_s),s)}\,ds}{\int_\Omega (1 + \int_0^t \delta_\alpha(\xi(x_s) - \xi')e^{\beta V_b(\xi(x_s),s)}\,ds)\,d\xi'}$$
$$= \frac{\int_{\mathcal{X}} \delta_\alpha(\xi(x) - \xi^*)e^{\beta(V(x)+C)}\,dx}{\int_\Omega \int_{\mathcal{X}} \delta_\alpha(\xi(x) - \xi')e^{\beta(V(x)+C)}\,dx\,d\xi'}$$
$$= e^{-\beta A_\alpha(\xi^*)}$$

The fact that, if a limit exists, then it is the correct one, is an important consistency check of the method. However, we were not able to prove that the biasing potential indeed converges (this seems difficult for ABP methods, while such an analysis can rigorously be done for some ABF methods[20]).

Let us now look more carefully at the first iterations of the algorithm, in order to understand the role of the constant c in eq 9 or eq 12. We base our considerations on the numerical discretization eq 13 to simplify the argument. First, recall that the constant c does not change the longtime limit of the algorithm. However, it helps accelerate the convergence during the initial transient regime. The first iteration of eq 13 indeed shows that

$$e^{\beta V_b(\xi^*,1)} = e^{\beta c}\frac{1 + \delta_\alpha(\xi(x_0) - \xi^*)e^{\beta c}}{1 + \delta_\alpha(0)e^{\beta c}}$$

When c is such that $e^{\beta c}$ is small, $V_b(\xi^*, 1)$ is raised by a small amount, and the gradient of V_b encourages trajectories to move away from ξ^* to some small extent. By increasing the value of c, we obtain a bias potential that pushes trajectories away from ξ^* more strongly, hence increasing the efficiency of the bias potential, in particular at the early stages of the process. We therefore conclude that the value of c should be as large as possible while maintaining numerical stability. Not all ABP methods update their biases according to this rule (see the comparison between our approach and the standard self-healing umbrella sampling (SHUS) algorithm in section 3.1).

To conclude this section, let us note that, once the bias is converged, it can be fixed and used as a bias to compute thermodynamic properties as in any importance sampling approach.

3. Comparison with Other Methods

3.1. Self-Healing Umbrella Sampling. SHUS[9] can be seen as a special case of the method presented here. SHUS can be written in terms of eq 12 using the following time-dependent constant:

$$e^{\beta c(n)} = \max_{\xi^*}[e^{-\beta A_\alpha(\xi^*,n)}]$$

With this choice we have $V_b = -A_\alpha$ and $\int_\Omega e^{\beta V_b(\xi,\,t)}\,d\xi = 1$. This choice for $c(n)$ appears to be suboptimal which may be related to the analysis of section 2.3.3 that shows that the value of c should be as large as possible. Notice also that, when the reaction coordinate space is discretized into a finite number of bins, the normalization condition eq 7 should be restated as a sum over bin indexes and the maximal value of $\exp[-\beta A_\alpha(\xi, n)]$ is therefore less than 1. This corresponds to a negative value of $c(n)$. We checked for the test case considered in section 4 that our method outperforms SHUS for precisely this reason.

3.2. Adaptive Biasing Force. We compare numerically our approach to two ABF formulations in section 4.1. ABF is a good reference for comparison because there are no model parameters to choose. Errors arise only through time and reaction coordinate discretization. Two exact formulations of the free energy gradient are eq 4 above, and

$$F(\xi^*) = -\left\langle \frac{d}{dt}\left(M_\xi \frac{d\xi}{dt}\right)\right\rangle_{\xi^*} \tag{15}$$

where $M_\xi^{-1} = JMJ^t$ with M being the mass matrix and J being defined in eq 4 (see ref 15 for this second expression). We point out that, in practice, $F(\xi)$ is approximated by a trajectory average $F(\xi, t)$, which is then used to bias the dynamics. For further details on the expressions eq 4 and eq 15 or their numerical implementation, we refer the reader to the cited works.

With ABF, one must address constructing the free energy from an estimation of its gradient, the calculated field F. While there are specific solutions to this problem[15,21,22] we employ a standard variational formulation. We recast this question as an optimization problem where the objective function

$$I(u) = \int_\Omega ||F(\xi) - \nabla_\xi u||^2\,d\xi \tag{16}$$

is to be minimized. The corresponding Euler−Lagrange equation is

$$\Delta_\xi u(\xi) = \nabla_\xi \cdot F \tag{17}$$

which is just Poisson's equation, to be supplemented with appropriate boundary conditions (depending on the problem at hand). The solution $u(\xi)$ is the best representation of the free energy given the vector field $F(\xi)$. This is solved via finite difference in the present work, but finite elements (or any Galerkin method) could be used as well.

3.3. Metadynamics. Because we have developed a method within the adaptive bias potential paradigm, we also make a comparison to well-tempered metadynamics.[23] In this formulation of metadynamics, the bias potential in one dimension is given by

$$V_b^{\mathrm{meta}}(\xi, \tau) = \sum_{t'\le\tau} G(\xi - \xi_{t'}, h(\xi, t'), w) \tag{18}$$

where the functions $G(X, H, W)$ are Gaussians of width W and height H, centered on X. We write V_b^{meta} to indicate that this is the bias potential generated by metadynamics. The Gaussian height in well-tempered metadynamics is both dependent on time and position along the reaction coordinate $h(\xi, t) = \omega \exp[-V_b^{\mathrm{meta}}(\xi, t)/k_B\Delta T]\tau_G$. For details of this version of metadynamics, we refer the reader to ref 23. We compare to this particular formulation because it requires less interaction with the user and a choice of parameter values is given in the cited reference.

4. Numerical Examples

4.1. Simulation Details and Results. Alanine dipeptide is a familiar system for benchmarking sampling methods.[15,21,23−26] Here, we employ AMBER with a half femtosecond time step, no constraints, solvent effects are modeled with the generalized

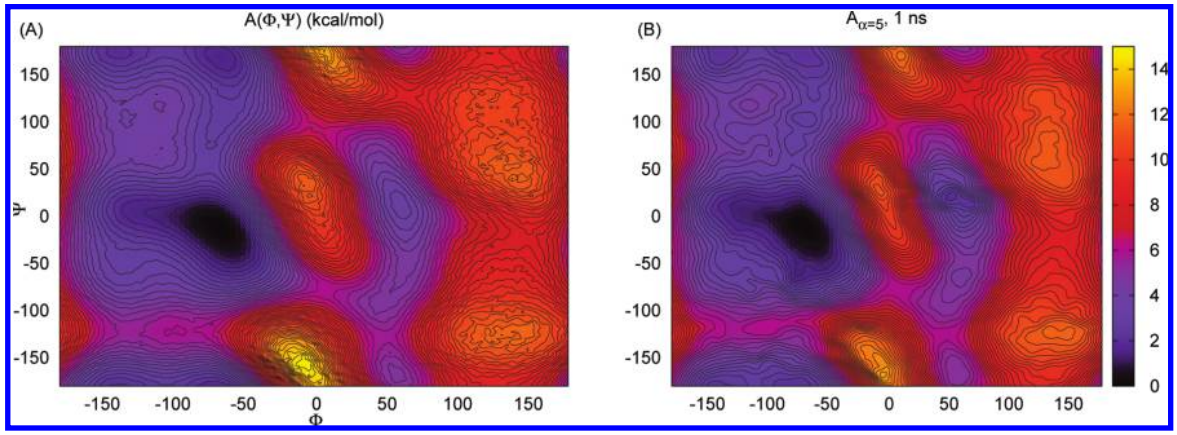

Figure 1. Contours are placed every $1/2k_BT$ (kcal/mol). (A) An estimate of the exact free energy (see text) which compares well to ref 15. (B) The free energy estimate after 1 ns of biased dynamics ($\alpha = 5$).

Born model, and we use the ff94 parametrization. The temperature was maintained at $T = 300$ K with Langevin dynamics where the collision frequency is 1 ps^{-1}. We select the common backbone dihedral angles $(\xi_1, \xi_2) = (\Phi, \Psi)$ as reaction coordinates.

When discretizing the reaction coordinate, it is common to use a small bin size to be sure that the free energy is correctly captured. Here, we use 300 bins of width 1.2°. We will also consider a bin width of 3.6° for eq 15 to examine the influence of bin size on ABF. In practice, for eqs 13 and 14, the current configuration along a trajectory may contribute only to an $m \times m$ grid centered around $(\xi_1(x_t), \xi_2(x_t))$, which amounts to truncating the range of the Gaussian function δ_α. The number of bins m were chosen so that $\delta'_\alpha(\xi - \xi^*)$ is negligible for ξ^* outside this box. For example, when $\alpha = 5°$ we use $m = 20$. In practice we neglect the normalization Z_n as well as the normalization of δ_α. We give a schematic algorithm in Appendix A.

In simulations with eqs 13, 4, and 15, we use a "ramp function" $R(N_{l,k}) = \min[1, N_{l,k}/N_0]$ to scale the biasing force (see, for instance, ref 15), where $N_{l,k}$ is the population in the bin (l, k) and the parameter $N_0 = 10$ was optimized for eqs 4 and 15. The ramp function scales the biasing force so that the initially noisy observations of the force do not induce nonequilibrium effects. The biasing force for the method presented here is given by eq 14. The biasing force for the ABF methods are given in eqs 4 and 15. The biasing forces (and biasing potential) are updated at each time step.

To study sampling efficiency we use the average difference

$$d(t) = \frac{1}{n^2}\sum_{k=1}^{n}\sum_{l=1}^{n}|A_{\mathrm{ref}}(k,l) - \hat{A}(k,l,t)| \qquad (19)$$

between the estimated free energy and a reference to be defined below. n is the number of bins in each coordinate, k and l are bin indices. For eqs 4 and 15 $\hat{A}$ is the solution of eq 17. In our method, $\hat{A}$ is either the left-hand side of eq 13, A_α, or its deconvoluted version $A_\alpha^{\mathrm{dcnvl}}$. Finally, for eq 18, $\hat{A} = -(T + \Delta T)V_b^{\mathrm{meta}}/\Delta T$. The reported results for $d(t)$ are found by using only a single trajectory with each method. We do not report the results obtained with SHUS since the convergence was found to occur much slower than for cases where $c > 0$.

We use the Richardson−Lucy algorithm[27,28] to deconvolute A_α because of its simplicity, but another method of deconvolution could be used, particularly if δ_α is not defined as a Gaussian. This algorithm is denoted by "RL" throughout. The RL algorithm uses the following iterative procedure:

$$f_{i+1}(\xi) = f_i(\xi)\int_\Omega \frac{e^{-\beta A_\alpha(\xi^*)}}{\int_\Omega \delta_\alpha(\hat{\xi} - \xi^*)f_i(\hat{\xi})\,d\hat{\xi}}\delta_\alpha(\xi^* - \xi)\,d\xi^* \qquad (20)$$

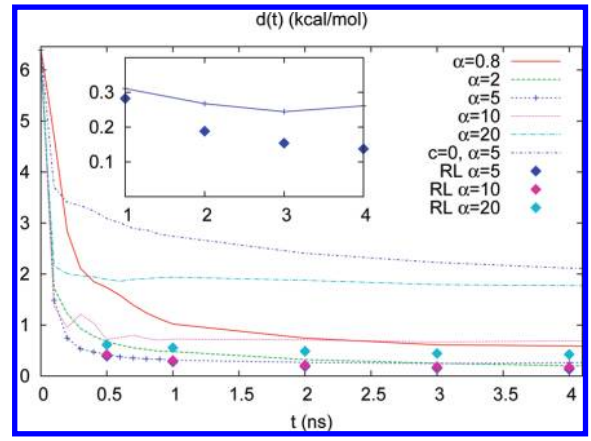

Figure 2. Error (eq 19) as a function of time for the method presented in this paper, for various α with and without deconvolution. Unless otherwise stated, $c = 15k_BT$. The $\alpha = 5$, $c = 0$ simulation demonstrates slow convergence due to a suboptimal choice of c, as described in the text. In the inset we show the last 4 ns of the $\alpha = 5°$ results.

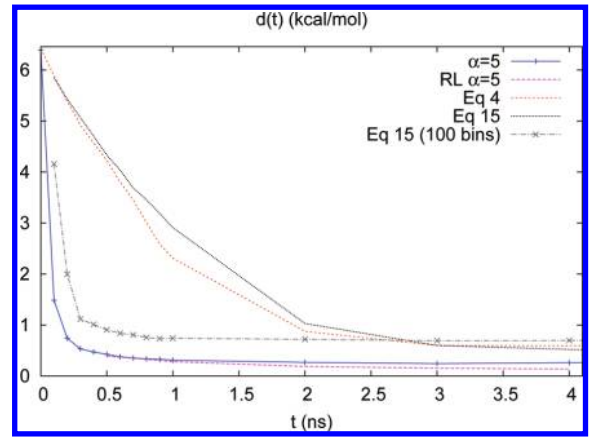

Figure 3. Error (eq 19) as a function of time for $\alpha = 5°$ and $\alpha = 10°$ with the method proposed in this paper, and comparison with ABF results obtained from eqs 4 and 15.

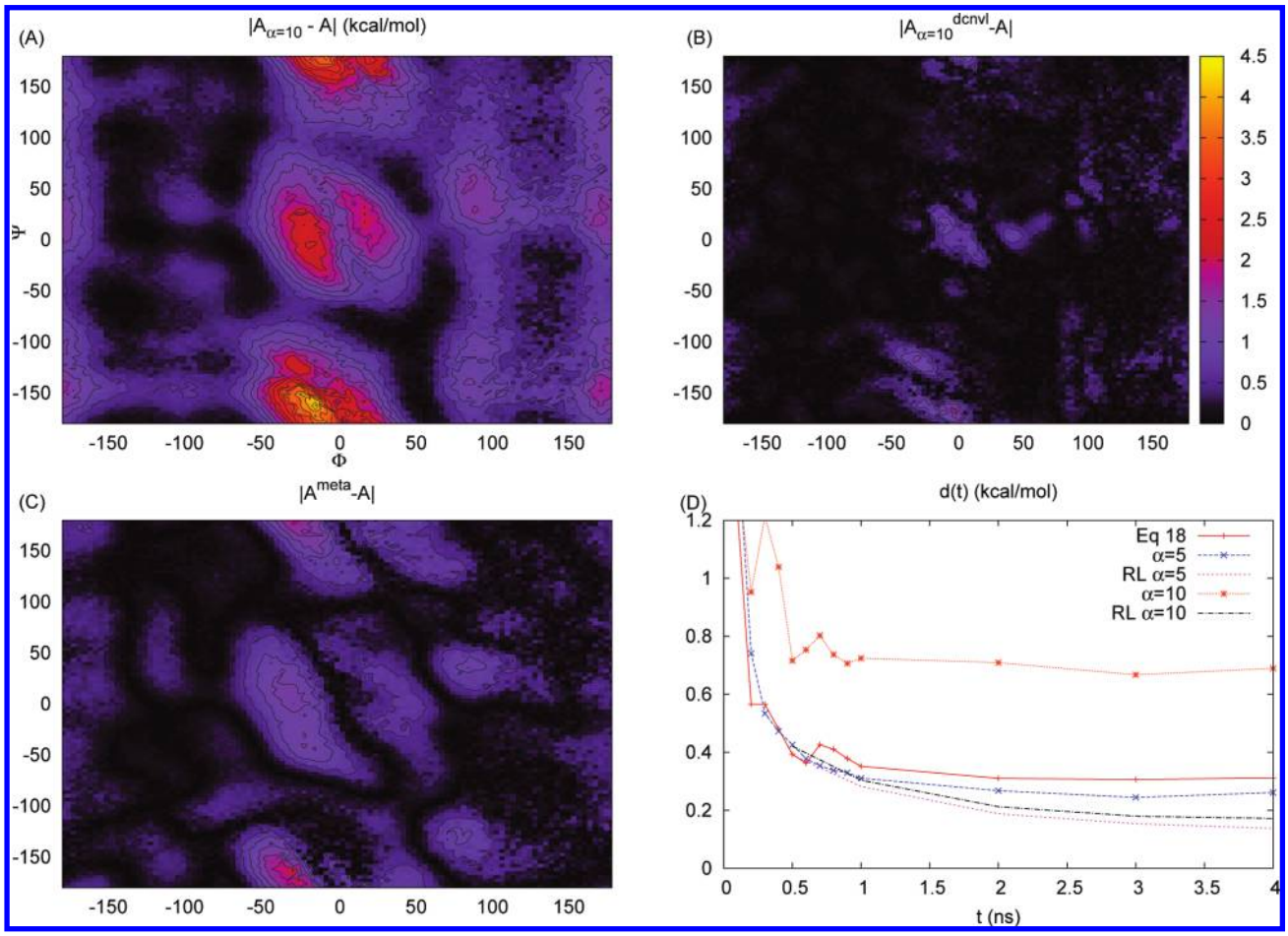

Figure 4. In panel A we show the absolute difference between the computed $A_{\alpha=10}$ and the reference A. Most of the error is, as expected, due to the regions of large curvature. In panel B the absolute difference between the deconvoluted free energy $A^{\mathrm{dcnvl}}_{\alpha=10}$ and the reference A is shown. In panel C we show the absolute difference between $A^{\mathrm{meta}} = -(T+\Delta T)V_b^{\mathrm{meta}}/\Delta T$ and the reference A. The free energy estimates in panels A−C were taken at the end of a 4 ns trajectory. In panel D eq 19 is shown for the well-tempered metadynamics method (eq 18) for comparison with results from the mollified DOS method.

where $f_0(\xi) = \exp[-\beta A_\alpha(\xi)]$, which is given by eq 13. To begin the algorithm, δ_α and f_i must be normalized. The fixed-point iteration eq 20 suggests that $f_n(\xi) \rightarrow \exp[-\beta A(\xi)]$ as $n \rightarrow +\infty$. We use 10 iterations in the reported results.

The reference free energy was computed by reweighting a long biased trajectory (120 ns) as

$$A_{\mathrm{ref}}(k,l) = -k_{\mathrm{B}}T \ln\Bigg(\sum_i \delta[\xi_k - \xi_1(x_i)] \times \delta[\xi_l - \xi_2(x_i)] \exp[\beta V_{\mathrm{b}}(\xi(x_i),\tau)] \Bigg)$$

where $V_b(\xi,\tau)$ was constructed from 4 ns of simulation with the mollified DOS method. The bias was not updated during the construction of the reference free energy. This produces a result free from errors associated with the choice of α. The reference profile A_{ref} is shown in Figure 1A, and in Figure 1B we show $A_\alpha(\xi,t)$ at 1 ns of sampling with $\alpha = 5°$. The average difference $d(t)$ is shown in 1 for A_α with different values of α. To show how the zero of energy of the bias potential controls the speed of convergence, in Figure 2 we plot eq 13 with $c = 0$ in eq 12 and we set $c = 15k_{\mathrm{B}}T$ for the remaining simulations. In Figure 3 we show $d(t)$ for eqs 4 and 15 (ABF methods). Results for eq 18 (well-tempered metadynamics) are shown in Figure 4D.

4.2. Efficiency of the Results As a Function of α. For small α, the nonlocality of the formulation disappears, and in Figure 2 we see slow convergence for $\alpha = 0.8°$. For intermediate values of α, nonlocality allows the bias potential to equilibrate much faster. For $\alpha = 2°$ and $\alpha = 5°$, A_α is a good approximation of A, $d(t)$ falls well under 1 kcal/mol, and we observe high efficiency. With the value $\alpha = 10°$, $d(t)$ plateaus at roughly 1 kcal/mol; α is now too large for A_α to be a good approximation of A. After applying the RL deconvolution to $A_{\alpha=10°}$, $d(t)$ drops to match the accuracy obtained with $\alpha = 2°$ or $\alpha = 5°$. The correspondence between A_α and A has deteriorated but not enough to decelerate the sampling: $A_{\alpha=10°}$ is still a good biasing potential and A can be recovered with deconvolution even at very short times.

For large α, eq 14 approaches zero, leaving only a small biasing force to accelerate the dynamics. To assess whether $\alpha = 20°$ is so large as to slow down the sampling, we apply the RL deconvolution. The results in Figure 2 demonstrate that A can be recovered to high accuracy for $\alpha = 20°$ at long times but that sampling efficiency is affected.

In Figure 3 we show $d(t)$ for eq 4 and eq 15 with a bin size of 1.2° and also for eq 15 with a bin width of 3.6°. If we compare the time to reach $d(t) = 1$ kcal/mol, simulation with eq 13 is roughly 3−10 times faster than that with eqs 4 and 15 for $2 \leq \alpha \leq 20$ at the bin size of 1.2°. For the larger bin size 3.6°, ABF sampling speed becomes competitive with the

mollified DOS approach, but it is impossible to remove the error. The 3.6° bin width coincides with the Gaussian half-width of δ_α when $\alpha = 2°$. A larger bin size can enhance sampling speed for ABF but at a cost in accuracy. Note that $\alpha = 20°$ corresponds to a δ_α with a half width that spans 33.3° in one dimension. This is a very large effective bin width for the accuracy of the results; a similar bin size with eq 4 or eq 15 would produce large, irreparable errors.

In Figure 4 we show results for the metadynamics simulations. We use the values $\Delta T = 1800$ K, $\omega = 0.24$ cal mol^{-1} fs^{-1}, and $\tau_G = 120$ fs, as suggested in ref 23. We could not improve the results by choosing different parameters. In panels A and B of Figure 4, we show the absolute difference between the computed $A_{\alpha=10}$ and the reference A with and without deconvolution, respectively. Clearly, the bulk of error is due to the misrepresentation of the very negatively curved regions of the free energy, and the ability to deconvolute A_α drastically reduces this error. In panel C we show the absolute difference between the free energy computed via eq 18 and the reference. We see again that the error is concentrated in the regions of large negative curvature but there is no simple and obvious way to reduce these errors with some postprocess. Panel D confirms that the metadynamics promotes extremely rapid sampling but that the long time accuracy, especially in strongly curved regions, is limited.

The results summarized in Figures 2, 3, and 4 imply that a wide range of values $2 \le \alpha \le 20$ lead to good efficiency. The ability to use the simple deconvolution algorithm is a clear advantage of the method.

4.3. Choosing α A Priori. We now discuss how to *a priori* choose α based on some rough error estimates. Taking ξ as a scalar, we may expand $e^{-\beta A(\xi^*)}$ as a Taylor series. Equation 3 yields

$$e^{-\beta(A_\alpha(\xi^*)-A(\xi^*))} \simeq 1 + \frac{\alpha^2}{4}\left[\left(\frac{A'(\xi^*)}{k_B T}\right)^2 - \frac{A''(\xi^*)}{k_B T}\right] \tag{21}$$

where we keep terms up to the second moment of δ_α. Assuming that $A(\xi)$ is harmonic near the minimum $\xi = q$, the curvature can be estimated as $A''(q) = k_B T/\sigma^2$, where σ^2 is the variance of the reaction coordinate at temperature T. From eq 21,

$$\exp[-\beta(A_\alpha(q) - A(q))] \simeq 1 - \frac{\alpha^2}{4\sigma^2}$$

While the higher order terms and the regions where $A' \neq 0$ are certainly important to the total error, this motivates defining α as a function of σ if little is known about the free energy; we can always calculate σ in the initial state.

We calculate the variance of the reaction coordinates to be about $\sigma^2 = 340$ deg^2 for both Φ and Ψ. In terms of the values of α discussed above, this implies that $\sigma/9 \le \alpha \le \sigma/2$ is a good range for fixing α from calculation of σ. Of course, different α′s may also be used for different coordinates.

5. Conclusion

In conclusion, we have developed and tested an efficient ABP scheme. The nonlocality of δ_α leads to a bias potential and a bias force that equilibrate rapidly. Shifting the zero of energy on the bias potential was shown to result in efficient importance sampling. The parameter c has influence on only the efficiency of the importance sampling but not on the limiting error of A_α. Because the bias potential is related to a convoluted free energy, deconvolution can be applied at the end of a simulation to remove all of the errors associated with the choice of the model parameter α - a unique feature and strength of this approach. This is limited only by the extent of sampling and the spacial discretization. This scheme easily accommodates the computation of the free energy surface and free energy gradient in several dimensions. We also suggest a simple means of *a priori* specifying α and c that should be quite general in applicability.

Acknowledgment. This work is supported by the Agence Nationale de la Recherche, under grants ANR-09-BLAN-0216-01 (MEGAS) and ANR-06-CIS-014 (SIRE).

A Schematic Algorithm

To help illustrate the simplicity of implementing eq 14 from the text

$$\frac{\partial A_\alpha(\xi^*, n+1)}{\partial \xi_j^*} = k_B T \frac{\sum_{i=0}^{n} \partial_{\xi_j^*}\delta_\alpha(\xi(x_i) - \xi^*) e^{\beta V_b(\xi(x_i),i)}}{1 + \sum_{i=0}^{n} \delta_\alpha(\xi(x_i) - \xi^*) e^{\beta V_b(\xi(x_i),i)}} \tag{22}$$

for a two-dimensional computation, we give a schematic algorithm here. We first define some array names. Let the array named "pop(k, l)" store the population at the (k, l) grid point (this is just the denominator of eq 22 above), where k corresponds to the bin index of $\xi_1(x_i)$ and l corresponds to the bin index of $\xi_2(x_i)$. Let the array named "dpop(j, k, l)" hold the derivative of the population along the $\xi_{j=1,2}$ direction at the point (k, l). The array "dpop" is simply the numerator of eq 22 above. We use "dA(k)" to store the gradient of the free energy at the present point (k, l). We assume that α has been calculated and c has been specified. We let $\delta_\alpha(\xi) = e^{-|\xi|^2/\alpha^2}$, which amounts to ignoring the normalization of the Gaussian functions. Lastly, we denote the trajectory in phase space as x_i, $F(n')$ is the force along the n'th degree of freedom, d/dn' is the derivative with respect to the n'th degree of freedom, and we use $V(x)$ for the potential energy.

First we initialize the arrays.

$$\begin{aligned} &t = 0, \ \ \mathrm{pop}(k,l) = 1 \quad \forall k,l \\ &\text{and} \ \ \mathrm{dpop}(j,k,l) = 0 \quad \forall k,l,j \\ &\text{and} \ \ M = 1 \end{aligned}$$

where $M = \max_{k,l}[\mathrm{pop}(k, l)]$. Each time the molecular dynamics forces are computed, we must also compute the current biasing information. Notice that we define everything in terms of the "pop" and "dpop" arrays so that no array is needed for the bias potential and that $M = \max_{k,l}[\mathrm{pop}(k, l)]$ can be updated without looping over the full reaction coordinate domain.

! evaluate free energy gradient at (k,l) for $j = 1,2$
$\mathrm{d}A(j) = \mathrm{dpop}(j,k,l)/\mathrm{pop}(k,l)$
! add bias forces to the existing forces and use a
! "Ramp function" R as described in the text
$R = \min(1,\mathrm{pop}(k,l)/10)$
$F(n') = F(n') + R \sum_{j=1}^{2} \mathrm{d}A(j)\, \mathrm{d}\xi_j/\mathrm{d}n'$
! evaluate the weighting factor W for updating "pop" and "dpop"

$W = \exp[\beta\ V_b] = \exp[\beta\ c]\mathrm{pop}(k,l)/M$
! update "pop" and "dpop" on an m by m grid
loop $k' = k - m/2,k + m/2$
  loop $l' = l - m/2,l + m/2$
    $\mathrm{pop}(k',l') = \mathrm{pop}(k',l') + \delta_\alpha(\xi_1(x_i) - \xi^*_{1,k'})\delta_\alpha(\xi_2(x_i) - \xi^*_{2,l'})W$
    if $\mathrm{pop}(k',l') > M$ then $M = \mathrm{pop}(k',l')$
    loop j = 1,2
      $\mathrm{dpop}(j,k',l') = \mathrm{dpop}(j,k',l') + \delta_{\xi_j}{}^*[\delta_\alpha(\xi_1(x_i) - \xi^*_{1,k'})\delta_\alpha(\xi_2(x_i) - \xi^*_{2,l'})]W$

We have defined k' and l' so that "pop" and "dpop" are updated on an $m \times m$ grid as discussed in the text. The treatment of (k', l') should reflect whether the domain is assumed to be periodic or not. The approximate free energy A_α is recovered (up to an additive constant) with $A_\alpha = k_B T \ln[\mathrm{pop}(k, l)/M]$.

The dynamics will now evolve in the presence of the biasing force $dA(j)$, while the arrays "pop" and "dpop" hold unbiased estimates of the population and the derivatives of the population. Notice that the free energy gradient is reduced to a simple ratio, and the only difficulty lies in the careful treatment of the loops over the grid points k' and l'. The often mathematically complex computation of the free energy and free energy gradient is reduced to simple bookkeeping.

References and Notes

(1) Hänggi, P.; Talkner, P.; Borkovec, M. *Rev. Mod. Phys.* **1990**, *62*, 251–341.
(2) Berg, B. A.; Neuhaus, T. *Phys. Lett. B* **1991**, *267*, 249–253.
(3) Berg, B. A.; Neuhaus, T. *Phys. Rev. Lett.* **1992**, *68*, 9–12.
(4) Hansmann, U.; Okamoto, Y.; Eisenmenger, F. *Chem. Phys. Lett.* **1996**, *259*, 321–330.
(5) Wang, F.; Landau, D. P. *Phys. Rev. E* **2001**, *64*, 056101:1−16.
(6) Wang, F.; Landau, D. P. *Phys. Rev. Lett.* **2001**, *86*, 2050–2053.
(7) Darve, E.; Pohorille, A. *J. Chem. Phys.* **2001**, *115*, 9169–9183.
(8) Laio, A.; Parrinello, M. *Proc. Natl. Acad. Sci. U.S.A.* **2002**, *99*, 12562–12566.
(9) Marsili, S.; Barducci, A.; Chelli, R.; Procacci, P.; Schettino, V. *J. Phys. Chem. B* **2006**, *110*, 14011–14013.
(10) Maragliano, L.; Vanden-Eijnden, E. *Chem. Phys. Lett.* **2006**, *426*, 168–175.
(11) Lelièvre, T.; Rousset, M.; Stoltz, G. *J. Chem. Phys.* **2007**, *126*, 134111:1–8.
(12) Zheng, L.; Yang, W. *J. Chem. Phys.* **2008**, *129*, 014105.
(13) Zheng, L.; Chen, M.; Yang, W. *Proc. Natl. Acad. Sci. U.S.A.* **2008**, *105*, 20227–20232.
(14) Zheng, L.; Chen, M.; Yang, W. *J. Chem. Phys.* **2009**, *130*, 234105.
(15) Darve, E.; Rodriguez-Gomez, D.; Pohorille, A. *J. Chem. Phys.* **2008**, *128*, 144120:1–13.
(16) Hansmann, U.; Eisenmenger, F.; Okamoto, Y. *Chem. Phys. Lett.* **1998**, *297*, 374–382.
(17) den Otter, W.; Briels, W. *J. Chem. Phys.* **1998**, *109*, 4139–4148.
(18) Sprik, M.; Ciccotti, G. *J. Chem. Phys.* **1998**, *109*, 7737–7744.
(19) Ciccotti, G.; Lelièvre, T.; Vanden-Eijnden, E. *Commun. Pure Appl. Math.* **2008**, *61*, 371–408.
(20) Lelièvre, T.; Rousset, M.; Stoltz, G. *Nonlinearity* **2008**, *21*, 1155–1181.
(21) Maragliano, L.; Vanden-Eijnden, E. *J. Chem. Phys.* **2008**, *128*, 184110:1–10.
(22) Kästner, J. *J. Chem. Phys.* **2009**, *131*, 034109:1−8.
(23) Barducci, A.; Bussi, G.; Parrinello, M. *Phys. Rev. Lett.* **2008**, *100*, 020603:1−4.
(24) Bartels, C.; Karplus, M. *J. Comput. Chem.* **1997**, *18*, 1450–1462.
(25) Strodel, B.; Wales, D. *Chem. Phys. Lett.* **2008**, *466*, 105–115.
(26) Li, X.; Latour, R. A.; Stuart, S. J. *J. Chem. Phys.* **2009**, *130*, 174106: 1–9.
(27) Richardson, W. *J. Opt. Soc. Am.* **1972**, *62*, 55–59.
(28) Lucy, L. *Astron. J.* **1974**, *79*, 745–754.

JP100926H